

Multiple bubble dynamics and velocity selection in Laplacian growth without surface tension

Mark Mineev-Weinstein*

New Mexico Consortium, Los Alamos, NM, 87544, USA;

Giovani L. Vasconcelos†

Departamento de Física, Universidade Federal do Paraná,

81531-990 Curitiba, Paraná, Brazil

Abstract

A new selection phenomenon in nonlinear interface dynamics is predicted. A generic class of exact regular unsteady multi-bubble solutions in a Hele-Shaw cell is presented. These solutions show that the case where the asymptotic bubble velocity, U , is twice greater than the velocity, V , of the uniform background flow, i.e., $U = 2V$, is the only attractor of the dynamics. Contrary to common belief, the predicted velocity selection requires neither surface tension nor other external regularization.

PACS numbers: 47.20.Hw, 47.20.Ma, 47.15.km, 02.30.Ik

* mark_mw@hotmail.com

† giovani.vasconcelos@ufpr.br

I. INTRODUCTION

Nonlinear interface dynamics and pattern formation out of equilibrium were and still are at the forefront of fundamental physics and remain also of great importance for numerous applications [1]. The Laplacian growth (LG), that is, interface motion under potential flow, is probably one of the deepest and at the same time the simplest and the most universal process of this kind, as it grasps all major features of unstable interface dynamics:

- nonlinearities;
- instabilities;
- formation of universal patterns;
- multiple applications, ranging from oil/gas recovery to malignant growth.

It also stands as the prototype for many growth processes, such as dendritic solidification [2], combustion fronts [1], electro-migration of voids [3], streamer ionization fronts [4], and bacterial colony growth [5], to name just a few. In addition, it has remarkable hidden integrable structure behind its mathematical formulation (see below).

The recent surge of interest in LG was motivated by the set of remarkable discoveries of deep connections of the LG problem with branches of fundamental physics, such as quantum gravity [6] and quantum Hall effect [7]. In addition, strong connections of LG with *mathematics* were revealed, on both the *classical* (the inverse potential problem [8], Riemann surfaces [9]) and *modern* levels (integrable hierarchies [10], random matrices [11], and the soliton theory of the hydrodynamic kind [9]).

The major challenge of LG interface dynamics in a Hele-Shaw channel (HSC), posed by Saffman and Taylor in 1958 [12], was the selection of a single observable pattern (mainly a finger or a bubble) from a continuum of stationary solutions obtained in the absence of surface tension (ST). Since then, this problem has been at the center of attention because of highly non-trivial physics and mathematics that defied traditional treatments. Since the problem was presented in [12], the invariably held common belief was that it is ST that selects the observable pattern. This belief was confirmed when, after considerable efforts in the 1980s, it was finally shown by several groups [13–16] that the inclusion of small ST indeed leads to the observable velocity selection. After these works the selection problem was considered to be resolved.

Quite surprisingly, it was shown later, first in [17] for a finger and later in [18, 20, 21]

for a bubble, that there is no need of ST (nor any other external regularization) for velocity selection in a HSC. In these works the velocity is selected entirely within the zero surface-tension (ZST) dynamics, by demonstrating that the selected pattern is the only attractor of the dynamical system describing the interface evolution. Since these works addressed only a single interface, it was not clear if selection without ST would hold for multiple interfaces. This article aims precisely to address selection for multiple interfaces. (Laplacian growth in multiply connected domains was considered earlier in [22] and [9], albeit in a different context.)

In [18] we conjectured (a) that our ZST selection mechanism works for an arbitrary number of bubbles, and (b) that all bubbles reach the same asymptotic velocity, which is precisely twice the velocity of the uniform background flow. In other words, $U = 2V$ in the long time limit, where U and V are the bubble and background flow velocities, respectively. Mathematical difficulties to describe multiple interfaces prevented us at that time to verify these two conjectures.

In this paper, we extend the exact ZST steady solutions for multiple interfaces in a HSC reported in [23] to the *unsteady* case. By using these new unsteady solutions, we demonstrate that any number of bubbles reach the same asymptotic velocity, $U = 2V$, thus proving a conjecture stated in [18]. This result contributes to both physics and mathematics. In physics, it predicts a novel effect, easily experimentally testable [24] and important for numerous applications. In mathematics, it presents a new rich class of unsteady exact solutions for a notoriously challenging problem—unstable nonlinear dynamics with infinite degrees of freedom. Thus, it also contributes to the field of integrable nonlinear systems — an intensively developing subdiscipline of mathematical physics.

A similar class of regular ZST solutions for a finger [25] faithfully reproduces the real dynamics observed in numerics in the low ST limit. But bubble dynamics in a Hele-Shaw cell is much less understood than finger evolution (see [26] for open problems in bubble dynamics). It is both tempting and important for science and applications to obtain exact solutions against which to compare experiments and simulations to remove any controversies (mostly induced by instabilities).

Below, we derive a rich class of unsteady non-singular multi-bubble ZST solutions. Obtaining these solutions is possible due to the integrability of the LG problem, which allows one to recast the problem as a set of *conservation laws*. The solutions are given in terms

of a conformal mapping from a canonical multiply connected domain (interior of the unit circle with a set of smaller disks removed) to the fluid region outside the bubbles. The mapping is written in closed form in terms of certain special transcendental functions — the secondary Schottky-Klein prime functions [27]. The Schottky-Klein prime functions were first used [28] to construct conformal mappings for multiply connected domains, and applied to several problems [29], including steady multiple bubbles in an unbounded Hele-Shaw cell [30]. Later, the secondary Schottky-Klein prime functions were introduced [27], which allowed to address multiple steady bubbles in a HSC [23]. Here we shall use the secondary Schottky-Klein prime functions to construct exact unsteady solutions for multiple bubbles in a HSC and study velocity selection in this context.

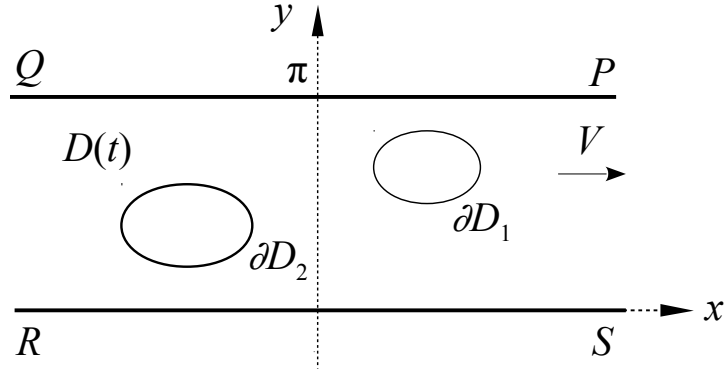
To address the velocity selection problem in the asymptotic regime, we need only solutions that stay regular for all times. Thus, we exclude initial data leading to solutions that cease to exist or lose univalence in finite time. In the theory of ill-posed problems, such data narrowing is known as Tikhonov regularization [31–35]. Then, the problem becomes well-posed, provided the data left after such removal are continuous w.r.t. all smooth initial data. This restricted set of data is called the *set of well-posedness* of the problem. Within the set of well-posedness, one deals only with regular solutions. After the Tikhonov regularization, one can study all aspects of this dynamical system, including the problem of selection *without surface tension or any other external regularization*.

The paper is organized as follows. We formulate the problem in Sec. II and obtain explicit unsteady solutions in Sec. III. In Sec. IV, we analyze the solutions for $t \rightarrow \infty$ and establish $U = 2V$ as the only attractor of the ZST dynamical system; we also review other selection mechanisms in the same section. All these results are summarized in Sec. V.

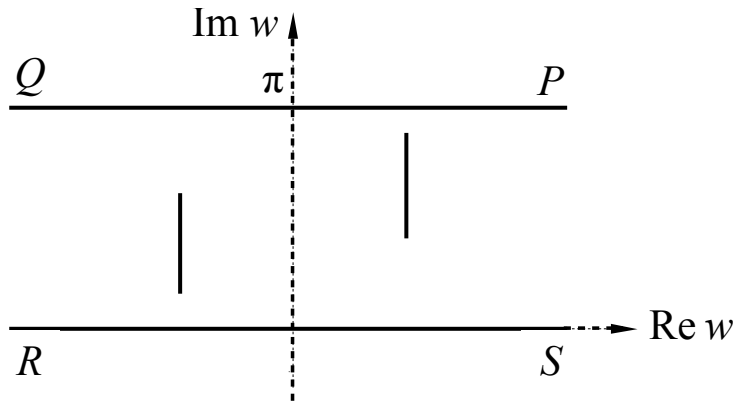
II. MATHEMATICAL FORMULATION

A. Multiple bubbles in a Hele-Shaw channel

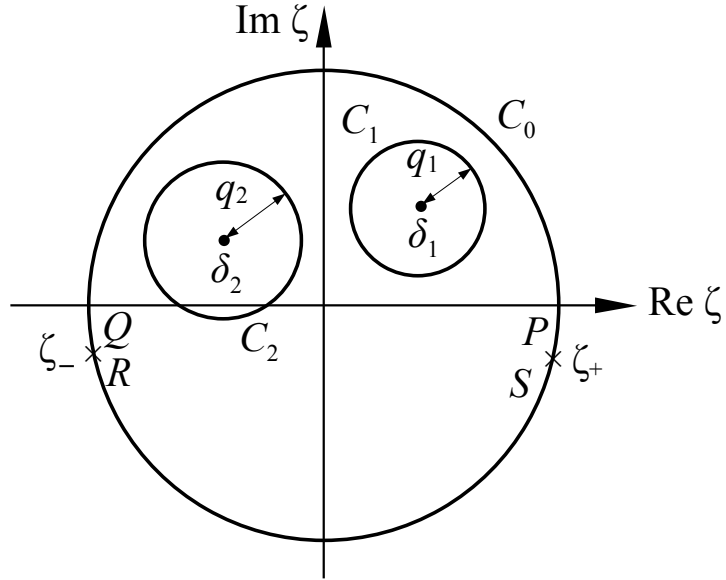
The Hele-Shaw channel is an infinite (in both directions) horizontal strip occupied by a viscous fluid (oil), denoted by the domain $D(t)$, and by M inviscid bubbles, represented by the non-intersecting domains $D_j(t)$, $j = 1, 2, \dots, M$, trapped inside the oil, as shown in Fig. 1a for $M = 2$. The uniform oil source at $x = -\infty$ pushes the flow toward the



(a)



(b)



(c)

Figure 1: The flow domains for a finite assembly of bubbles in a Hele-Shaw channel: (a) the physical z -plane; (b) the w -plane of the complex potential; and (c) the auxiliary complex ζ -plane. The points ζ_{\pm} in the ζ -plane are mapped to $x = \pm\infty$ in the z -plane.

uniform sink at $x = +\infty$. The problem is formulated (in scaled units where the channel width is chosen to be π and the background velocity V is set to unity) as follows. As oil is incompressible, i.e., $\text{div } \mathbf{v} = 0$, where \mathbf{v} is the oil velocity vector field, and the flow is potential, $\mathbf{v} = -\text{grad } p$ (Darcy's law), where p is pressure, we obtain the 2D Laplace equation: $\nabla^2 p = 0$. It also follows from above that $\lim_{x \rightarrow \pm\infty} p = -x$. Also, $\partial_n p = 0$ (no normal flow) at the channel boundaries, $y = 0$ and $y = \pi$, where ∂_n is the normal derivative. In addition, we have $p = p_j(t)$ along the moving interface $\partial D_j(t)$, for $j = 1, \dots, M$, where the p_j 's are constant along the bubble boundaries, since pressure is constant inside the bubbles and ST is neglected. Finally, the kinematic boundary condition requires that the normal velocities of the moving boundary, V_n , and of the oil, v_n , coincide, so $V_n = -\partial_n p$ at the moving interface $\Gamma(t) = \bigcup_j \partial D_j$. The full mathematical formulation of the problem thus takes the following form:

$$\begin{cases} \nabla^2 p = 0 & \text{in } D(t), & (1a) \\ p = p_j & \text{at } \partial D_j(t), & (1b) \\ V_n = -\partial_n p & \text{at } \Gamma(t), & (1c) \\ p = -x & \text{for } x \rightarrow \pm\infty, & (1d) \\ \partial_n p = 0 & \text{at } y = 0 \text{ and } y = \pi. & (1e) \end{cases}$$

The goal is to find closed form solutions of (1) for the unsteady dynamics of an *arbitrary* number of inviscid droplets. Earlier solutions [18] were restricted to a single interface. To deal with multiple bubbles we must recast the problem in terms of conformal mappings between multiply connected domains. Let us note that Laplacian growth in multiply connected domains is not completely specified by the initial configuration only [9], since it is necessary to prescribe additional conditions from which one can determine the pressures p_j . Rather than specify *a priori* the pressures p_j , we shall instead fix certain geometric parameters of the conformal mapping, so as to ensure that the p_j 's remain constant in time; see Sec. III B.

B. The conformal mapping

Let us solve (1a)–(1e) using a conformal mapping $z(\zeta, t)$ from a special domain in an auxiliary complex ζ -plane to the oil domain $D(t)$. Since $\nabla^2 p = 0$ we introduce a complex potential $w(z, t) = -p(x, y; t) + i\psi(x, y; t)$, analytic in $D(t)$ and subject to boundary

conditions indicated below.

All three complex planes, z , ζ , and w , mentioned above, are shown in Fig. 1 for the case $M = 2$ (i.e., two bubbles). The physical plane $z = x + iy$, see Fig. 1a, represents the oil with M bubbles, $D_j(t)$ ($j = 1, \dots, M$), moving to the right together with the oil. The oil domain, $D(t)$, occupies the horizontal strip, $0 < y < \pi$, excluding the bubbles regions, $D_j(t)$. The complex potential w -plane is shown in Fig. 1b. The vertical slits there represent the bubble boundaries, $\partial D_j(t)$, and the horizontal lines describe the north/south walls of the channel:

$$\begin{cases} \operatorname{Re} w = -p = -p_j, \\ \operatorname{Im} w = \psi = 0, \pi, \end{cases}$$

where the first condition indicates isobars in accordance with (1b) and the second one stands for streamlines in accordance with (1e).

The complex plane, $\zeta = \xi + i\eta$, used for the conformal map $z(\zeta, t)$, is shown in Fig. 1c. The oil domain D_ζ in the ζ -plane corresponds to the interior of the unit circle C_0 , with M disjoint circles, C_j , $j = 1, \dots, M$, excised from it. Here δ_j and q_j are the center and the radius of the j -th circle. The circles C_j are mapped to the bubble boundaries, $\partial D_j(t)$, in the z -plane and to the vertical slits in the w -plane, whereas C_0 is mapped to the channel walls, $y = 0, \pi$, in the z -plane and to $\psi = 0, \pi$ in the w -plane, while the points $\zeta_\pm \in C_0$ are respectively mapped to the sink and source at $x = \pm\infty$. For uniqueness of conformal mapping between two given domains, we fix the following three real parameters: $\delta_1 = 0$, so that the circle C_1 is concentric with C_0 , and $\zeta_+ = 1$. (We shall, however, keep the symbol ζ_+ in the formulas below for convenience of notation.)

Let us double the flow domain $D(t) \rightarrow D(t) \cup \overline{D(t)}$, where bar denotes complex conjugation, so adding a new set of bubbles within this extended domain, which are the mirror reflections of $D_j(t)$ with respect to the real axis. Similarly, the extended domain in the ζ -plane, to be denoted by F_0 , is obtained by adding to D_ζ its reflection in the unit circle C_0 :

$$F_0 = D_\zeta \cup \varphi_0(D_\zeta), \quad (2)$$

where $\varphi_0(\zeta) = 1/\bar{\zeta}$ denotes reflection in C_0 . The planar domains D_ζ and $\varphi_0(D_\zeta)$ can be seen as the two halves of the Riemann surface (Schottky double) [9, 36] obtained by ‘‘gluing’’ each circle C_j to its reflection, $C_{-j} = \varphi_0(C_j)$, in C_0 (see [27, 28]).

For later use, let us introduce the following Moebius maps:

$$\theta_j(\zeta) = \delta_j + \frac{q_j^2 \zeta}{1 - \delta_j \zeta}, \quad j = 1, \dots, M, \quad (3)$$

whose inverses are

$$\theta_{-j}(\zeta) \equiv \theta_j^{-1}(\zeta) = \frac{1}{\overline{\theta_j(1/\zeta)}}, \quad (4)$$

where $\bar{f}(\zeta)$ denotes the Schwarz conjugate of $f(\zeta)$ defined by $\bar{f}(\zeta) = \overline{f(\bar{\zeta})}$. One can verify that $\theta_j(\zeta)$ maps the interior of the circle C_{-j} onto the exterior of the circle C_j . The set Θ_0 consisting of all compositions of the maps θ_j and their inverses defines a classical Schottky group and the region F_0 defined in (2) is a fundamental region of the group Θ_0 [37].

Of particular interest to us here is the subgroup $\Theta_M \subset \Theta_0$ that consists of only and all *even* combinations of the maps θ_j , $j = 1, \dots, M$, and their inverses. For some $1 \leq l \leq M$, let us then consider the set of $2M - 1$ Möbius maps, ψ_k , defined by

$$\psi_k \equiv \theta_l \circ \theta_k, \quad k = -M, \dots, M, \quad k \neq 0, -l. \quad (5)$$

These maps are fundamental generators of the subgroup Θ_M , and the same group Θ_M is generated irrespective of the choice of l [27]. Associated with the Schottky group Θ_M , one can define certain special transcendental functions, known as the secondary Schottky-Klein prime functions $\Omega_M(\zeta, \alpha)$, see Appendix A, in terms of which the solution for $z(\zeta, t)$ will be given in Sec. III.

C. Symmetry relations

Equation (1e) implies that the conformal map $z(\zeta, t)$ satisfies the following boundary condition:

$$\text{Im}[z(\zeta, t)] = \text{constant}, \quad \text{for } \zeta \in C_0. \quad (6)$$

Using that $\bar{\zeta} = 1/\zeta$ for $\zeta \in C_0$, we can recast (6) as

$$\bar{z}(1/\zeta, t) = z(\zeta, t) + \text{constant} \quad \text{or} \quad \bar{z}(1/\zeta, t) \simeq z(\zeta, t), \quad (7)$$

where $h(z) \simeq f(z)$ means that $h(z) = f(z) + \text{constant}$. Equation (7) is valid for $\zeta \in C_0$ and elsewhere by analytic continuation. Another symmetry relation for $z(\zeta, t)$ can be obtained by considering the boundary conditions at the bubble interfaces, as shown below.

We note that equations (1a)–(1c) are equivalent to

$$\mathcal{S}_t = 2w_z, \quad (8)$$

where subscripts are partial derivatives and $\mathcal{S}(z, t)$ is the Schwarz function [38, 39] of the curve $\Gamma(t)$, defined as $\bar{z} = \mathcal{S}(z, t)$ for $z \in \Gamma(t)$. It follows from (8) that all singularities of $\mathcal{S}(z, t)$ in $D(t)$ different from those of $w(z)$ are constants of motion [39].

One can show that the Schwarz function of the j -th bubble boundary ∂D_j has the following representation in the ζ -plane

$$g_j(\zeta, t) \equiv \mathcal{S}_j(z(\zeta, t), t) = z(\theta_{-j}(\zeta), t) \quad (9)$$

(see Appendix B). The Schwarz functions $g_j(\zeta, t)$, $j = 1, \dots, M$, differ only by constants,

$$g_k(\zeta, t) = g_j(\zeta, t) + G_{kj}, \quad (10)$$

where G_{kj} may depend on time but not on ζ . In other words, the Schwarz functions $\mathcal{S}_j(z, t)$ computed from each individual boundary ∂D_j can be seen as different logarithmic branches of the global Schwarz function $\mathcal{S}(z, t)$. Now, from (8) and the boundary conditions on $w(z, t)$, it follows that $\mathcal{S}_j(z, t)$ has constant imaginary part on the channel walls or alternatively: $\text{Im}[g_j(\zeta, t)] = \text{constant}$ for $\zeta \in C_0$. This, together with (7) and (9), implies (see Appendix B) that

$$g_j(\zeta, t) \simeq z(\theta_j(\zeta), t). \quad (11)$$

From (9)–(11) we then obtain the following important symmetry relations:

$$z(\psi_k(\zeta), t) \simeq z(\zeta, t), \quad (12)$$

where $\psi_k = \theta_l \circ \theta_k$, for a fixed l and $k = -M, \dots, M$, with $k \neq 0$. Since the maps $\psi_k(\zeta)$ are generators of the group Θ_M , see (5), Eq. (12) states that $z(\zeta, t)$ is invariant (up to an additive constant) under each element of Θ_M . In other words, $z(\zeta, t)$ is an *additive automorphic function* [40] with respect to the group Θ_M . This property is crucial to constructing exact solutions to the problem of multiple bubbles in a HSC, as will be seen next.

III. EXACT TIME-DEPENDENT SOLUTIONS

In what follows, we address *non-singular* solutions, which remain finite for all times. Among other advantages, these solutions enable us to solve the selection problem in the long-time asymptotics. In other words, we leave aside solutions that blow up in finite

time, either by developing cusps or losing univalence, as physically non-realizable. In this way we regularize this initially ill-posed problem, that is, we convert it into a well-posed one (see more details in Sec. III B). But first, we would like to present a rich class of *unsteady* non-singular multi-bubble solutions by extending earlier results [17] (fingers) and [18] (single bubble). This class describes all smooth initial data with any desirable degree of accuracy. (It is well known that ratios of polynomials, i.e., rational functions or so-called Padé approximants, provide a complete description of all smooth curves [19]. Since linear combination of logarithms, which is our solutions, is an integral of rational functions with simple poles, whose sum give the most generic Padé approximants, this explains why our solution given by (15) describes any smooth curve as close as desired.)

A. The complex potential

The following formula links the complex potential $W(\zeta, t) \equiv w(z(\zeta, t), t)$ and our *key* function, $\Omega_M(\zeta, \alpha)$ (see (30) and [23]):

$$W(\zeta, t) = \log \frac{\Omega_M(\zeta, \zeta_-) \Omega_M(\zeta, \theta_l(\zeta_+))}{\Omega_M(\zeta, \zeta_+) \Omega_M(\zeta, \theta_l(\zeta_-))} + i c_l(t), \quad (13)$$

where l can be $1, 2, \dots, M$, and $c_l(t)$ is a real constant [41]. Using the properties of $\Omega_M(\zeta, \alpha)$ given in Appendix A (or in [23]), one can verify that $W(\zeta, t)$ satisfies the desired boundary conditions (1b) and (1e), which in this case read:

$$\begin{cases} \operatorname{Re}[W(\zeta, t)] = -p_j = \text{constant}, & \text{for } \zeta \in C_j, \\ \operatorname{Im}[W(\zeta, t)] = \text{constant}, & \text{for } \zeta \in C_0. \end{cases}$$

If ζ in C_l we find that

$$p_l = \log \left| \frac{\delta_l - \zeta_+}{\delta_l - \zeta_-} \right|. \quad (14)$$

We shall henceforth set $l = 1$, which implies $p_1 = 0$, since $\delta_1 = 0$. Thus, the pressure on the bubble surface ∂D_1 is taken as the reference pressure with respect to which the pressures in the other bubbles are measured. Furthermore, setting $\delta_1 = 0$ in (3) yields $\theta_1(\zeta) = q_1^2 \zeta$.

B. Exact Unsteady Solutions

As we want to study selection in the asymptotic regime, we must deal exclusively with solutions $z(\zeta, t)$ that remain non-singular for all times. This restriction to initial data leading

to non-singular solutions is known as Tikhonov regularization of ill-posed problems, whereby the well-posedness of the problem may be ensured by narrowing the class of possible initial data to an appropriate set, called the *set of well-posedness* of the problem [33, 34]. By extending non-singular solutions from simpler geometries [17-19] to the case of multiple bubbles, we have found that the solutions in all these cases have the same form: $z(\zeta, t)$ is the sum of time-dependent *logarithms* (see below).

In terms of the Schotky-Klein formalism, the solution for $z(\zeta, t)$ takes the form

$$z(\zeta, t) = h(t) + i\Delta + \log \frac{\Omega(\zeta, \zeta_-)}{\Omega(\zeta, \zeta_+)} + \alpha_0 \log \frac{\Omega(\zeta, q_1^2 \zeta_+)}{\Omega(\zeta, q_1^2 \zeta_-)} + \sum_{k=1}^N [\alpha_k \log \Omega(\zeta, a_k) + \bar{\alpha}_k \log \Omega(\zeta, 1/\bar{a}_k)], \quad (15)$$

where the subscript from Ω_M has been dropped to save space. Here the function $h(t)$ and constants Δ and α_0 are real (with $|\alpha_0| < 1$), $a_k(t) \notin F_0$ are complex [see (2) to recall the definition of the fundamental region F_0], and the complex constants α_k satisfy

$$\sum_{k=1}^N \alpha_k = 0, \quad (16)$$

to ensure that $z(\zeta, t)$ is single-valued. Without loss of generality, the values of $a_k(0)$ are chosen to be inside the circle C_1 and outside the circle obtained by the inversion of C_0 in C_1 , i.e., $q_1^2 < |a_k| < q_1$. The quantity Δ in (15) can be determined from the condition that $\text{Im}[z(\zeta, t)] = 0$ for ζ on the lower segment of the unit circle, as shown in Fig. 1 [42].

When $M = 1$, Eq. (15) reproduces a single bubble dynamics [18]. In this case, the circular domain D_ζ becomes an annulus, and the Schottky-Klein prime functions are reduced to Jacobi theta functions [29], in terms of which the solution for a single bubble was expressed in [18]. For more than one bubble ($M > 1$) one must employ the full-fledged secondary prime functions.

Making use of properties of $\Omega(\zeta, \alpha)$ [see Appendix A], one can verify that $z(\zeta, t)$ given in (15) satisfies the required symmetry relations (7) and (12). One also sees from (13) and (15) that $w(z) \approx z$ for $|z| \rightarrow \infty$, as required by (1d). Furthermore, the moving boundary of the j -th bubble is given by $\partial D_j(t) = z(\delta_j + q_i e^{i\varphi}, t)$, where $\varphi \in [0, 2\pi]$ parametrizes the bubble boundaries. To find the time dependency of $a_k(t)$ and $h(t)$ in (15), we shall consider a set of conserved quantities of the dynamics.

First let us consider the conserved singularities of the Schwarz function $\mathcal{S}(z, t)$. From (11) we obtain that

$$g_1(\zeta, t) = h(t) + i\Delta' + \log \frac{\Omega(q_1^2 \zeta, \zeta_-)}{\Omega(q_1^2 \zeta, \zeta_+)} + \alpha_0 \log \frac{\Omega(\zeta, \zeta_+)}{\Omega(\zeta, \zeta_-)} + \sum_{k=1}^N [\alpha_k \log \Omega(q_1^2 \zeta, a_k) + \bar{\alpha}_k \log \Omega(q_1^2 \zeta, \bar{a}_k)], \quad (17)$$

where in writing the term containing α_0 we used that $\Omega(q_1^2 \zeta, q_1^2 \alpha) = q_1^2 \Omega(\zeta, \alpha)$; see relation (42) in Appendix A. Here Δ' is a real-valued quantity whose expression is not relevant for our discussion. Recalling that the a_k 's are inside C_1 but outside the reflection of C_0 in C_1 , meaning that $q_1^2 < |a_k| < q_1$, it follows from (17) that the only singularities of $g_1(\zeta, t)$ in D_ζ are the points $\zeta_k = \varphi_0(a_k) = q_1^2/\bar{a}_k$, for $k = 1, \dots, N$. This implies, in turn, that the only singularities of $\mathcal{S}(z, t)$ in the fluid domain $D(t)$ are located at the points β_k , where

$$\beta_k = z(q_1^2/\bar{a}_k, t), \quad k = 1, \dots, N. \quad (18)$$

More explicitly, we have

$$\beta_k = h(t) + i\Delta + \log \frac{\Omega(q_1^2/\bar{a}_k, \zeta_-)}{\Omega(q_1^2/\bar{a}_k, \zeta_+)} + \alpha_0 \log \frac{\Omega(1/\bar{a}_k, \zeta_+)}{\Omega(1/\bar{a}_k, \zeta_-)} + \sum_{m=1}^N [\alpha_m \log \Omega(q_1^2/\bar{a}_k, a_m) + \bar{\alpha}_m \log \Omega(q_1^2/\bar{a}_k, 1/\bar{a}_m)]. \quad (19)$$

Since all singularities of $\mathcal{S}(z, t)$ within $D(t)$ are constants of motion, we have $\dot{\beta}_k = 0$, where dot denotes time derivative. *Analytically*, the β_k 's are the logarithmic, time-independent singularities of the Schwarz function, $\mathcal{S}(z, t)$, located in $D(t)$, while *geometrically* they are vertices of virtual fjords [43], akin to those in [44, 45].

We can obtain a second set of conserved quantities by analyzing the asymptotic behavior of $\mathcal{S}(z, t)$ for $x \rightarrow \pm\infty$. First, it follows from (17) that if $\alpha_0 \neq 0$ then $g_1(\zeta, t)$ has logarithmic singularities at ζ_\pm :

$$g_1(\zeta, t) \approx \pm\alpha_0 \log(\zeta - \zeta_\pm) + h(t) + B_\pm(t), \quad \zeta \rightarrow \zeta_\pm, \quad (20)$$

so $\mathcal{S}(z, t)$ behaves for $x \rightarrow \pm\infty$ as

$$\mathcal{S}(z, t) = -\alpha_0 z + \frac{2}{U} h(t) + C_\pm(t) + O\left(\frac{1}{z}\right), \quad (21)$$

where

$$U = \frac{2}{1 + \alpha_0}. \quad (22)$$

and $C_{\pm}(t)$ remain finite for all times. (The time-dependency of $B_{\pm}(t)$ and $C_{\pm}(t)$ are irrelevant for the present discussion.) From $\lim_{|x| \rightarrow \infty} w_z = 1$ and (8), it follows that $\lim_{|x| \rightarrow \infty} \mathcal{S}_t(z, t) = 2$, so by virtue of (21) the quantities

$$\beta_{\pm} = \frac{2}{U} h(t) - 2t + C_{\pm}(t) \quad (23)$$

are constant in time, i.e., $\dot{\beta}_{\pm} = 0$. One can show that $\text{Im}[\beta_+] = \text{Im}[\beta_-]$, hence there are only three independent real quantities for the two complex constants β_{\pm} .

The total area A of the bubbles can be neatly expressed through the constants β_k and β_{\pm} as

$$\frac{A}{\pi} = \frac{\beta_+ - \beta_-}{2} + \text{Re} \sum_{k=1}^N \bar{\alpha}_k \beta_k, \quad (24)$$

and so A is guaranteed to remain constant throughout the evolution. However, we do not have analytical formulas for the areas, A_j , of the individual bubbles.

As discussed in [9], multi-bubble LG requires $M - 1$ additional relations to determine the pressures p_j , for $j = 2, \dots, M$ (recall that we have set $p_1 = 0$ as a reference pressure). One can fix either the bubble pressures p_j or the bubble areas A_j . In either case we have $2N + M + 2$ conserved real quantities: N complex β_k ($k = 1, \dots, N$), β_{\pm} (recalling that $\text{Im}[\beta_+] = \text{Im}[\beta_-]$), and A_j (or p_j), for $j = 2, \dots, M$. We can enforce these conditions by keeping δ_j , for $j = 2, \dots, M$, fixed in time and solving for the remaining $2N + M + 2$ real parameters: N complex parameters a_k and $M + 2$ real parameters, namely h , $\gamma_- = \arg(\zeta_-)$, and q_j , $j = 1, \dots, M$. (Recall that we have used the three degrees of freedom of the Riemann mapping theorem to set $\delta_1 = 0$ and $\zeta_+ = 1$.) As explicit formulas for A_j and p_j are either not available or hard to deal with numerically, we fix both δ_j and q_j , for $j = 2, \dots, M$, in time. Then we are left with $2N + 3$ real free parameters: N complex a_k and real γ_- , h , and q_1 . There is equal number of conserved real quantities: $N + 2$ complex β_k and β_{\pm} , subject to $\text{Im}[\beta_+] = \text{Im}[\beta_-]$.

The conservation laws (19) and (23) provide (implicitly) the full dynamics of the conformal mapping $z(\zeta, t)$, thus completing the description of generic unsteady motion for multiple

bubbles. Initial conditions should be chosen carefully to avoid possible finite-time singularities due to formation of cusps or loss of univalence (in short, to avoid finite time blow ups). Fortunately, there is a large set of such initial data. A simple rule to choose such favorable initial data is to place the β_k 's either behind the bubbles or clearly out of the bubbles' reach, so that these points are all left behind in the long-time limit and the solution approaches a steady regime. (If a bubble gets too close to one of the β_k 's the interface might eventually self intersect, which means that the solution blows up in finite time.) We note, however, that determining the bubbles' evolution for a given initial data requires solving numerically a set of nonlinear algebraic equations with transcendental special Schottky functions — a difficult task that we plan to address in the near future. In this context, it is perhaps worth mentioning that in the simpler case of a single bubble, where the solutions are written in terms of well-known elliptic functions, several numerical examples of interface evolution have been reported [20].

After we have presented the full dynamics in Eqs. (19) and (23), let us now focus on the long-time limit ($t \rightarrow +\infty$) in order to address the velocity selection — the main goal of this article.

C. Long-time Asymptotics

Let us now consider the asymptotic behavior of the solution (15) for $t \rightarrow \infty$. From (23) one sees that in order to keep β_{\pm} fixed in time we must have $h(t) \rightarrow Ut$, for $t \rightarrow \infty$, since all other terms remain finite in this limit. Similarly, the divergence of $h(t)$ must be cancelled in (19) by a divergent logarithmic term, since β_k must remain constant for all times. This divergence cancelation can only arise from the third term in the RHS of (19), so we need $q_1^2/\bar{a}_k \rightarrow \zeta_-$ for $t \rightarrow \infty$. This implies that all a_k 's must approach the point $q_1^2\zeta_-$ when $t \rightarrow +\infty$, and they do so exponentially slow:

$$a_k(t) = q_1^2\zeta_- + c_k e^{-\lambda_k t}, \quad (25)$$

where $\text{Re}[\lambda_k] > 0$ and c_k are asymptotic constants. (The expressions for λ_k and c_k are too lengthy and irrelevant for the present argument.)

In this limit and since $\sum_k \alpha_k = 0$, the solution (15) reduces to

$$z(\zeta, t) = Ut + \log \frac{\Omega(\zeta, \zeta_-)}{\Omega(\zeta, \zeta_+)} + \left(1 - \frac{2}{U}\right) \log \frac{\Omega(\zeta, q_1^2\zeta_-)}{\Omega(\zeta, q_1^2\zeta_+)}, \quad (26)$$

where a nonsignificant additive constant was omitted. In other words, in the long-time asymptotics the assembly of M bubbles reaches a steady regime where all bubbles move to the right with the velocity U [23]. This result holds regardless of the conditions imposed to determine the pressures $p_j(t)$, as it is based only on the conserved quantities β_k and β_{\pm} , defined in (19) and (23).

We have thus succeeded to extend the steady solutions for multiple bubbles obtained in [23] to the *unsteady* regime, which is a crucial step to address velocity selection.

IV. VELOCITY SELECTION

A. Selection for fingers and single bubbles: Brief review

As mentioned in the Introduction, the most challenging aspect of the Hele-Shaw interface dynamics is the *selection problem*, posed in 1958 by Saffman and Taylor in their seminal work [12] on viscous fingering in a HSC. They observed that the asymptotic shape (the finger) reaches a width that is exactly one half of the channel width (or equivalently the finger velocity U is twice the velocity V of the background flow of the viscous fluid, i.e., $U = 2V$). In the same work [12], a continuous family of stationary solutions for all values $0 < U < \infty$ was found. Then why only the value $U = 2V$ from this continuous family is observed (or selected)? The answer to this problem, conjectured in [12], attributed the observed selection to surface tension (ST), which is neglected in the continuum family of exact solutions. But the authors of [12] were unable to confirm this conjecture because of mathematical difficulties to include ST.

The reason of these difficulties (which also occurred in subsequent attempts of this kind) is that ST, here denoted by σ , is a singular perturbation in this problem. In other words, the value $\sigma = 0$ is an essential singularity of the mapping function $z(\zeta, t)$. Therefore this function cannot be expanded as a power series of ST near zero, and so ST cannot be used for a regular perturbation treatment.

In 1984 Kruskal and Segur [46] found a remedy to overcome this difficulty by treating (exponentially) small ST corrections of the finger shape. They developed “asymptotics beyond all orders” [47], which is a variation of the well known quasiclassical (also called WKB) approach in quantum mechanics. The role of a small Planck constant \hbar in WKB

is played by (also small) σ in the selection problem. Using this approach several groups [13–16] showed in the mid 1980s that inclusion of ST switches the continuous spectrum mentioned above to a discrete countable family, all of which converge to $U = 2V$ when ST approaches zero. The same approach was also applied to a single *bubble* in a HSC [48, 49] whereby it was shown that the same velocity $U = 2V$ is selected. With these works, the long-standing conjecture that ST causes selection was finally confirmed and the beyond-all-orders asymptotic analysis was accepted as the solution to the selection problem. The dynamical selection for multifingers has been considered in [50]. See also [51] for a survey (up to 2004) of the selection problem in Hele-Shaw flows.

The commonly accepted wisdom that ST is necessary for selection was unexpectedly challenged in 1998, when the observed finger was selected without ST [17]. Using a general class of exact unsteady non-singular solutions, it was possible to show that the steady solution with $U = 2V$ is the only attractor of the dynamics. This analysis [17] demonstrated that the special nature of the solution with $U = 2V$ is already present (or “built in”) in the zero surface tension Laplacian growth, in agreement with selection by inclusion of surface tension and other regularizations. Indeed, in later works it was theoretically found [52], and numerically confirmed [53], that other boundary conditions, such as kinetic undercooling [52], also lead to the same $U = 2V$ selection. More strikingly, similar selection has also been observed experimentally in non-fluid systems, such as finger-like ionization fronts in electric breakdown [4], where there is no analog of ST, thus confirming that external regularizations are not necessary for velocity selection. Alternative attempts to get selection without surface tension have been made by maximizing some function of the pattern shape [54] and by considering a finite channel flow [55], although it was subsequently argued in [56] that finite size effects are irrelevant for both selection and the interface dynamics far from boundaries.

More recently, the velocity selection $U = 2V$ was demonstrated (again without ST) for a single bubble [18, 20, 21], using an approach similar to that used for a finger [17]. In [18], a new family of *unsteady* solutions for a single bubble in a channel helped to demonstrate that $U = 2V$ is the only stable fixed point (attractor) of this dynamical system. The same result was obtained for a single bubble in an unbounded cell [21]. In this work, by extending the unsteady dynamics from a single to an arbitrary number of bubbles, we arrive to the same selection, $U = 2V$, as discussed next.

B. Velocity selection for multiple bubbles

From Eqs. (19) and (23) for the full time dynamics of the singularities it follows that there are two fixed points for the $a_k(t)$'s: $q_1^2\zeta_-$ (shown to be an attractor in Sec. III C) and $q_1^2\zeta_+$. The second fixed point $q_1^2\zeta_+$ is, on the contrary, a repeller, as shown next.

Recall from Sec. III B that if we initially have a map $z(\zeta, 0)$ with singularities at $a_0^\pm(0) = q_1^2\zeta_\pm$, i.e., $\alpha_0 \neq 0$ in (15), then such a configuration (provided it exists for all times) will evolve to a steady regime with $U \neq 2$. Let us now perturb the initial configuration by displacing slightly this singularities from $q_1^2\zeta_\pm$: i.e., $a_0^\pm(0) = q_1^2\zeta_\pm + \varepsilon_\pm$, when $|\varepsilon_\pm| \ll 1$, while $a_k(0)$, for $k = 1, \dots, N$, stay intact. Then the term containing α_0 in (15) takes the form

$$\frac{\alpha_0}{2} \log \frac{\Omega(\zeta, q_1^2\zeta_+ + \varepsilon_+) \Omega(\zeta, 1/(q_1^2\zeta_+^{-1} + \bar{\varepsilon}_+))}{\Omega(\zeta, q_1^2\zeta_- + \varepsilon_-) \Omega(\zeta, 1/(q_1^2\zeta_-^{-1} + \bar{\varepsilon}_-))}, \quad (27)$$

which is chosen to preserve the symmetry relations (7) and (12). Under the above perturbation, initial singularities at the fixed points $q_1^2\zeta_\pm$ are shifted to non-fixed points $q_1^2\zeta_\pm + \varepsilon_\pm$, which must then move to the point $q_1^2\zeta_-$ for $t \rightarrow +\infty$ (see Sec. III C), implying that

$$\begin{cases} \varepsilon_+ \rightarrow q_1^2(\zeta_- - \zeta_+), \\ \varepsilon_- \rightarrow 0, \end{cases}$$

or more completely

$$a_0^\pm(t) = q_1^2\zeta_\pm + \varepsilon_\pm(t) = q_1^2\zeta_- + O(\exp(-\lambda_\pm t)), \quad t \rightarrow +\infty, \quad (28)$$

where $\text{Re } \lambda_\pm > 0$. Thus, the term (27) approaches zero asymptotically.

Since all other singularities $a_k(t)$ also move to $q_1^2\zeta_-$, the sum in (15) vanishes, so we arrive at the following asymptotic solution:

$$z(\zeta, t) = 2t + \log \frac{\Omega(\zeta, \zeta_-)}{\Omega(\zeta, \zeta_+)}. \quad (29)$$

Thus, the bubble assembly reaches the velocity $U = 2$ in the steady regime. This result establishes that the only stable fixed point (attractor) for the $a_k(t)$'s describing an arbitrary number of moving bubbles in the channel corresponds to $U = 2$.

V. CONCLUSION

We have presented a new class of exact solutions (15) for unsteady motion of an assembly of inviscid bubbles in a Hele-Shaw channel when surface tension is neglected. The solution

was constructed in terms of a conformal mapping from a canonical multiply connected domain to the viscous fluid region outside the bubbles. This mapping was obtained in closed form in terms of the secondary Schottky-Klein prime function introduced in [27]. In this way, we solved in quadrature the initial value problem for multiple bubbles in a channel.

This means that we have converted the differential equations for the problem (1a)–(1e) to algebraic-like equations for the constants of motion (19) and (23) which fully govern the dynamics of the mapping singularities a_k 's. Then, given initial values of all a_k 's ($k = 0, 1, \dots, N$) in the set of well-posedness of the problem (see above), our solutions (15) remain non-singular for all times and thus describe the multi-bubble evolution for $0 \leq t < \infty$. Since any initial shape can be expressed in terms of our logarithmic class of solutions with any desirable accuracy (because logarithms are integrals of rational functions with simple poles which can approximate any smooth function), it means that we solved the problem exactly and completely. This became possible because of integrability of our non-linear initial value problem. Finding specific numerical solutions for a given initial data is a more challenging problem that is left for the future, as it is outside the scope of the present work. We note in passing, however, that in the simpler case of a single bubble several numerical examples have been reported [20] where the solutions display many of the features discussed here in the more general multibubble setting.

After obtaining the full multi-bubble dynamics, we analyzed the long-time regime ($t \rightarrow +\infty$), in order to address the velocity selection problem — the main physical result of our paper. (The details of the pre-asymptotic dynamics is an interesting topic for future work.) We have shown that in the long-time asymptotics the assembly of bubbles reaches the same velocity, $U = 2V$, which is precisely twice the background uniform flow velocity, V , provided by the source (and sink) at $|x| \rightarrow \infty$. Our results thus show that within the generalized class of non-singular solutions, the steady solution with $U = 2V$ is the only attractor of the time-dependent dynamics. This confirms our conjecture stated earlier in [18] that $U = 2V$ should be selected irrespective of the number of bubbles. The predicted phenomena is expected to be observed in experiments and probably cannot be described analytically by more traditional mathematical tools.

It is instructive to compare the dynamical selection mechanism discussed above with the standard approach to the selection problem via regularization of the Saffman-Taylor problem by including surface tension. In the latter, it was shown via asymptotics beyond

all orders that only a discrete set of steady solutions survive the regularization procedure and that all such solutions converge to $U = 2V$ when surface tension approaches zero. This selection by surface tension was limited to the steady-state framework, thus leaving aside the pre-asymptotic stages; while our ZST selection describes the whole evolution of arbitrary interfaces for $0 \leq t < \infty$. Also, by revealing the instability (without surface tension) of all continuum of steady solutions except for $U = 2V$, we significantly clarified the dynamical origin of velocity selection in LG. Here we have extended for multiple interfaces the approach originated in [17, 18] for a single interface.

G.L.V. is grateful to the Department of Mathematics at the Imperial College in London, where this work was initiated. M.M-W. acknowledges the Brazilian agency CAPES for financial support and thanks both the Department of Physics at UFPE, Brazil, and the Simons Center for Geometry and Physics for hospitality during intermediate stages of the work. G.L.V. acknowledges partial funding from Conselho Nacional de Desenvolvimento Científico e Tecnológico (Brazil) under Grant No. 312985/2020-7.

APPENDIX A: THE SCHOTTKY-KLEIN PRIME FUNCTIONS

Associated with the Schottky subgroup Θ_M introduced in Sec. II B, one can define the secondary Schottky-Klein prime functions $\Omega_M(\zeta, \alpha)$ as follows [27]:

$$\Omega_M(\zeta, \alpha) = (\zeta - \alpha) \prod_{\psi \in \Theta_M''} \frac{(\zeta - \psi(\alpha))(\alpha - \psi(\zeta))}{(\zeta - \psi(\zeta))(\alpha - \psi(\alpha))}. \quad (30)$$

where $\Theta_M'' \subset \Theta_M$ is the set such that for all $\psi \in \Theta_M$, excluding the identity, either ψ or ψ^{-1} (but not both) is contained in Θ_M'' .

The function $\Omega_M(\zeta, \alpha)$ satisfies the following functional identity [27]:

$$\frac{\Omega_M(\psi_k(\zeta_1), \gamma_1)}{\Omega_M(\psi_k(\zeta_2), \gamma_2)} = \frac{\tilde{\beta}_j(\gamma_1, \gamma_2)}{\tilde{\beta}_j(\zeta_1, \zeta_2)} \sqrt{\frac{\psi_k'(\zeta_1) \Omega_M(\zeta, \gamma_1)}{\psi_k'(\zeta_2) \Omega_M(\zeta, \gamma_2)}}, \quad (31)$$

where we recall that $\psi_k = \theta_l \circ \theta_k$, for a fixed l and $k = -M, \dots, M, k \neq 0, l$, with $\theta_j(\zeta)$ as defined in (3), are generators of the group Θ_M . Here

$$\tilde{\beta}_k(\zeta, \gamma) = \exp[2\pi i (\tilde{v}_j(\zeta) - \tilde{v}_j(\gamma))], \quad (32)$$

where the functions $\tilde{v}_k(\zeta)$ are $2M - 1$ integrals of the first kind on the Riemann surface associated with the Schottky group Θ_M [37]. Two particular cases of (31) are of interest

here. For $\zeta_1 = \zeta_2 = \zeta$ we have

$$\frac{\Omega_M(\psi_k(\zeta), \gamma_1)}{\Omega_M(\psi_k(\zeta), \gamma_2)} = \tilde{\beta}_k(\gamma_1, \gamma_2) \frac{\Omega_M(\zeta, \gamma_1)}{\Omega_M(\zeta, \gamma_2)}, \quad (33)$$

while for $\psi_1(\zeta) = \theta_1^2(\zeta) = q_1^4 \zeta$ and $\gamma_1 = \gamma_2 = \gamma$ we get

$$\frac{\Omega_M(q_1^4 \zeta_1, \gamma)}{\Omega_M(q_1^4 \zeta_2, \gamma)} = \tilde{\beta}_1(\zeta_2, \zeta_1) \frac{\Omega_M(\zeta_1, \gamma)}{\Omega_M(\zeta_2, \gamma)}, \quad (34)$$

which implies that

$$\frac{\Omega_M(q_1^2 \zeta_1, \gamma)}{\Omega_M(q_1^2 \zeta_2, \gamma)} = \tilde{\beta}_1(\zeta_2/q_1^2, \zeta_1/q_1^2) \frac{\Omega_M(\zeta_1/q_1^2, \gamma)}{\Omega_M(\zeta_2/q_1^2, \gamma)}. \quad (35)$$

If we now define the function

$$F(\zeta; \gamma_1, \gamma_2) = \log \frac{\Omega_M(\zeta, \gamma_1)}{\Omega_M(\zeta, \gamma_2)}, \quad (36)$$

it then follows from (33) that $F(\zeta; \gamma_1, \gamma_2)$ is additive automorphic with respect to the group Θ_M :

$$F(\psi_k(\zeta); \gamma_1, \gamma_2) \simeq F(\zeta; \gamma_1, \gamma_2). \quad (37)$$

where we recall that the equality sign \simeq means that the two functions (on each side of the sign) differ at most by an additive constant.

The function $\Omega_M(\zeta, \alpha)$ also satisfies the following symmetry relation [27]:

$$\overline{\Omega}_M(\phi_j(\zeta), \phi_j(\alpha)) = -\frac{q_j^2}{(\zeta - \delta_j)(\alpha - \delta_j)} \Omega_M(\zeta, \alpha), \quad (38)$$

for $j = 0, 1, \dots, M$, where we defined

$$\overline{\Omega}_M(\zeta, \alpha) \equiv \overline{\Omega_M(\zeta, \alpha)},$$

and $\phi_j(\zeta)$ is the conjugation map on circle C_j , i.e., $\bar{\zeta} = \phi_j(\zeta)$ for $\zeta \in C_j$, which can be written as

$$\phi_j(\zeta) = \bar{\theta}_j(1/\zeta) = \frac{1}{\theta_{-j}(\zeta)}. \quad (39)$$

In particular, for $j = 0$ relation (38) simplifies to

$$\overline{\Omega}_M(1/\zeta, 1/\alpha) = -\frac{1}{\zeta\alpha} \Omega_M(\zeta, \alpha). \quad (40)$$

Alternatively, taking the complex conjugate of (38) and using (39) and (40) we obtain

$$\Omega_M(\theta_j(\zeta), \theta_j(\alpha)) = \frac{q_j^2}{(1 - \bar{\delta}_j \zeta)(1 - \bar{\delta}_j \alpha)} \Omega_M(\zeta, \alpha). \quad (41)$$

For the particular case $j = 1$, we have

$$\Omega_M(q_1^2 \zeta, q_1^2 \alpha) = q_1^2 \Omega_M(\zeta, \alpha). \quad (42)$$

where we recall that the circle C_1 was chosen concentric with the unit circle, so that $\delta_1 = 0$ and $\theta_1(\zeta) = q_1^2 \zeta$.

APPENDIX B: SYMMETRY RELATIONS FOR $z(\zeta, t)$

The Schwarz function $\mathcal{S}_j(z, t)$ of an interface ∂D_j has the following representation in the ζ -plane:

$$g_j(\zeta, t) \equiv \mathcal{S}_j(z(\zeta, t), t) = \overline{z(\zeta, t)} = \bar{z}(\bar{\zeta}, t), \quad \zeta \in C_j. \quad (43)$$

Upon using that $\bar{\zeta} = \phi_j(\zeta)$ for $\zeta \in C_j$ and (39), one obtains

$$g_j(\zeta, t) = \bar{z}(1/\theta_{-j}(\zeta), t), \quad (44)$$

which is valid for $\zeta \in C_j$ and elsewhere by analytic continuation. Using (7) into (44), we then get

$$g_j(\zeta, t) = z(\theta_{-j}(\zeta), t), \quad (45)$$

which recovers (9).

Next, it follows from (8), and the boundary conditions on $w(z, t)$, that $\mathcal{S}_j(z, t)$ must have constant imaginary part on the channel walls: $\text{Im}[\mathcal{S}_j(z, t)] = \text{constant}$, for $y = 0, \pi$. This implies in turn that $\text{Im}[g_j(\zeta, t)] = \text{constant}$ for $\zeta \in C_0$, or more compactly

$$\overline{g_j(\zeta, t)} \simeq g_j(\zeta, t), \quad \zeta \in C_0. \quad (46)$$

Considering the particular case $\zeta \in C_0$ in (45) and using (39) and (7), we obtain that

$$\overline{g_j(\zeta, t)} = \bar{z}(1/\theta_j(\zeta), t) = z(\theta_j(\zeta), t), \quad \zeta \in C_0. \quad (47)$$

Combining (46) and (47) we thus have that

$$g_j(\zeta, t) \simeq z(\theta_j(\zeta), t), \quad (48)$$

which is valid on C_0 and elsewhere by analytic continuation. This proves relation (11).

Since different branches, $\mathcal{S}_j(z, t)$, of the Schwarz function can differ only by an additive constant, see (10), we can combine (45) and (48) as a single general relation:

$$z(\theta_j(\zeta), t) \simeq z(\theta_{-k}(\zeta), t). \quad (49)$$

Equivalently, we have

$$z(\theta_j \circ \theta_k(\zeta), t) \simeq z(\zeta, t). \quad (50)$$

Since $\psi_k = \theta_l \circ \theta_k$, for a fixed l , are generators of the group Θ_M , see (5), we thus conclude that

$$z(\psi(\zeta), t) \simeq z(\zeta, t), \quad \psi \in \Theta_M, \quad (51)$$

thus showing that $z(\zeta, t)$ is an additive automorphic function with respect to Θ_M , as anticipated in Sec. II C.

APPENDIX C: PROOF OF (14)

To show that the complex potential $W(\zeta, t)$ given in (13) has constant real part on the circles C_j , $j = 1, \dots, M$, let us first consider the case $j = l$. Using that $\bar{\zeta} = \phi_l(\zeta)$ for $\zeta \in C_l$, and the fact $\phi_j(\zeta) = \bar{\theta}_j(1/\zeta)$, we obtain that

$$\begin{aligned} \overline{\left(\frac{\Omega_M(\zeta, \theta_l(\zeta_+))}{\Omega_M(\zeta, \theta_l(\zeta_-))} \right)} &= \frac{\bar{\Omega}_M(\phi_l(\zeta), \phi_l(\zeta_+))}{\bar{\Omega}_M(\phi_l(\zeta), \phi_l(\zeta_-))} \\ &= \left(\frac{\delta_l - \zeta_-}{\delta_l - \zeta_+} \right) \frac{\Omega_M(\zeta, \zeta_+)}{\Omega_M(\zeta, \zeta_-)}, \end{aligned}$$

where in the last passage we used (38). Inserting this relation into (13) we have

$$W(\zeta, t) = \log \left[\overline{\left(\frac{\delta_l - \zeta_-}{\delta_l - \zeta_+} \right) \frac{Z}{\bar{Z}}} \right] + i c_l, \quad \zeta \in C_l, \quad (52)$$

where

$$Z = \frac{\Omega(\zeta, \zeta_-)}{\Omega(\zeta, \zeta_+)}.$$

It then follows from (52) that

$$p_l(t) = -\operatorname{Re} [W(\zeta, t)] \Big|_{\zeta \in C_l} = \log \left| \frac{\delta_l - \zeta_+}{\delta_l - \zeta_-} \right|,$$

thus obtaining (14).

Similarly, noting that $\theta_l = \psi_{-j}\theta_j$, where $\psi_{-j} = \theta_l \circ \theta_{-j}$ is a generator of the group Θ_M [see (5)], and using the transformation property (33), one can show that for $\zeta \in C_j$, $j \neq l$, one has

$$p_j(t) = -\operatorname{Re} [W(\zeta, t)] \Big|_{\zeta \in C_j} = \log \left| \frac{\delta_j - \zeta_+}{\delta_j - \zeta_-} \right| + 2\pi \operatorname{Im} [\tilde{v}_{-j}(\theta_j(\zeta_-)) - \tilde{v}_{-j}(\theta_j(\zeta_+))],$$

where $\tilde{v}_{-j}(\zeta)$ is the integral of first kind associated with the map ψ_{-j} . This result, together with (14), thus shows that the complex potential $W(\zeta, t)$ has constant real part on all circles C_j , $j = 1, \dots, M$, as required.

-
- [1] P. Pelcé, *Dynamics of Curved Fronts* (Academic Press, San Diego, 1988).
- [2] J. S. Langer, Instabilities and pattern formation in crystal growth, *Rev. Mod. Phys.* **52**, 1 (1980).
- [3] M. Ben Amar, Void electromigration as a moving free-boundary value problem, *Physica D* **134**, 275 (1999).
- [4] A. Luque, F. Brau, and U. Ebert, Saffman-Taylor streamers: mutual finger interaction in spark formation, *Phys. Rev. E* **78**, 016206 (2008).
- [5] J. Müller and W. Saarloos, Morphological instability and dynamics of fronts in bacterial growth models with nonlinear diffusion, *Phys. Rev. E* **65**, 061111 (2002).
- [6] M. Mineev-Weinstein, P. B. Wiegmann, and A. Zabrodin, Integrable structure of interface dynamics, *Phys. Rev. Lett.* **84**, 5106 (2000).
- [7] O. Agam, E. Bettelheim, P. Wiegmann, and A. Zabrodin, Viscous fingering and the shape of an electronic droplet in the quantum hall regime, *Phys. Rev. Lett.* **88**, 236801 (2002).
- [8] B. Gustafsson and A. Vasil'ev, *Conformal and Potential Analysis in Hele-Shaw Cell* (Birkhäuser, Basel, 2006).
- [9] I. Krichever, M. Mineev-Weinstein, P. Wiegmann, and A. Zabrodin, Laplacian growth and Whitham equations of soliton theory, *Physica D* **198**, 1 (2004).

- [10] I. K. Kostov, I. Krichever, M. Mineev-Weinstein, P. B. Wiegmann, and A. Zabrodin, The τ -function for analytic curves. In *Random Matrices and Their Applications*, MSRI Publ., Vol. 40, pp. 285-299, Ed. by P. Bleher and A. Its, Cambridge University Press, 2001.
- [11] M. Mineev-Weinstein, M. Putinar, and R. Teodorescu, Random matrices in 2D, Laplacian growth and operator theory, *J. Phys. A* **41**, 263001 (2008).
- [12] P. G. Saffman and G. I. Taylor, The penetration of a fluid into a porous medium or Hele-Shaw cell containing a more viscous liquid, *Proc. R. Soc. London, Ser. A* **245**, 312 (1958).
- [13] B. I. Shraiman, Velocity selection and the Saffman-Taylor problem, *Phys. Rev. Lett.* **56**, 2028 (1986).
- [14] D. C. Hong and J. S. Langer, Analytic theory of the selection mechanism in the Saffman-Taylor problem, *Phys. Rev. Lett.* **56**, 2032 (1986).
- [15] R. Combescot, T. Dombre, V. Hakim, Y. Pomeau, and A. Pumir, Shape selection of Saffman-Taylor fingers, *Phys. Rev. Lett.* **56**, 2036 (1986).
- [16] S. Tanveer, Analytic theory for the selection of a symmetric Saffman-Taylor finger in a Hele-Shaw cell, *Phys. Fluids* **30**, 1589 (1987).
- [17] M. Mineev-Weinstein, Selection of the Saffman-Taylor finger width in the absence of surface tension: an exact result, *Phys. Rev. Lett.* **80**, 2113 (1998).
- [18] G. L. Vasconcelos and M. Mineev-Weinstein, Selection of the Taylor-Saffman bubble does not require surface tension, *Phys. Rev. E* **89**, 061003(R) (2014).
- [19] G. A. Baker and P. Graves-Morris, *Padé Approximants*, Cambridge University Press, 1996.
- [20] G. L. Vasconcelos, A. Brum, and M. Mineev-Weinstein, Bubble dynamics in a Hele-Shaw cell: Exact solutions and the dynamical mechanism for velocity selection, arXiv:1910.04327 (2019).
- [21] A. H. Khalid, N. R. McDonald, and J. M. Vanden-Broeck, On the motion of unsteady translating bubbles in an unbounded Hele-Shaw cell, *Phys. Fluids* **27**, 012102 (2015).
- [22] S. Richardson, Hele-Shaw flows with time-dependent free boundaries in which the fluid occupies a multiply-connected region, *Eur. J. Appl. Math.* **5**, 97 (1994); Hele-Shaw flows with time-dependent free boundaries involving a concentric annulus, *Phil. Trans. R. Soc. Lond. A* **354**, 2513 (1996); Hele-Shaw flows with time-dependent free boundaries involving a multiply-connected fluid region, *Eur. J. Appl. Math.* **12**, 571 (2001).
- [23] G. L. Vasconcelos, Multiple bubbles and fingers in a Hele-Shaw channel: complete set of steady solutions, *J. Fluid Mech.* **780**, 299 (2015).

- [24] The group led by Profs. H. L. Swinney and E. L. Florin at the Center for Nonlinear Dynamics of the Department of Physics at Univ. of Texas started experiments with bubbles in a Hele-Shaw channel in order to verify our prediction that $U = 2V$.
- [25] A. Sarkissian and H. Levine, Comment on “Selection of the Saffman-Taylor Finger Width in the Absence of Surface Tension: An Exact Result”, *Phys. Rev. Lett.*, **81**, 4528 (1998).
- [26] K. Okumura, Viscous dynamics of drops and bubbles in Hele-Shaw cells: Drainage, drag friction, coalescence, and bursting, *Adv. Colloid Interface Sci.*, **225**, 64 (2018).
- [27] G. L. Vasconcelos, J. S. Marshall, and D. G. Crowdy, Secondary Schottky-Klein prime functions associated with multiply connected planar domains, *Proc. Roy. Soc. A* **471**, 20140688 (2014).
- [28] D. G. Crowdy. The Schwarz-Christoffel mapping to bounded multiply connected polygonal domains, *Proc. Roy. Soc. A* **461**, 2653 (2005).
- [29] D. G. Crowdy, E. H. Kropf, C. C. Green, and M. M. S. Nasser, The Schottky-Klein prime function: a theoretical and computational tool for applications. *IMA J. Appl. Math.*, **81**, 589 (2016).
- [30] D. G. Crowdy, Multiple steady bubbles in a Hele-Shaw cell, *Proc. Roy. Soc. A*, **465**, 421 (2009).
- [31] A. N. Tikhonov, On the stability of inverse problems, *Doklady Acad. Sci. USSR* **39**, 176–179 (1943); On the solution of ill-posed problems and the method of regularization, *Dokl. Akad. Nauk SSSR* **151**, 501–504 (1963) (in Russian); On the regularization of ill-posed problems. *Dokl. Akad. Nauk SSSR* **153**, 49–52 (1963) (in Russian).
- [32] A. N. Tikhonov and V. Ya. Arsenin, *Solutions of Ill-Posed Problems* (Wiley, New York, 1977).
- [33] V. K. Ivanov, V. V. Vasin, V. P. Tanana, *Theory of Linear Ill-Posed Problems and its Applications* (De Gruyter, Berlin, Boston, 2013)
- [34] M. M. Lavrent’ev, V. G. Romanov, and S. P. Shishatskii, *Ill-Posed Problems of Mathematical Physics and Analysis*, Series: Translations of Mathematical Monographs, Vol. 64 (American Mathematical Society, 1986)
- [35] S. I. Kabanikhin, *J. Inv. Ill-Posed Problems* **16**, 317–357 (2008).
- [36] M. Schiffer and D.C. Spencer, *Functionals of finite Riemann surfaces* (Princeton University Press, 1954).
- [37] H. F. Baker, *Abelian functions: Abel’s theorem and the allied theory of theta functions* (Cam-

- bridge University Press, Cambridge, 1897).
- [38] P. J. Davis, *The Schwarz Function and its Applications*, Carus Mathematical Monograph No. 17, The Mathematical Association of America, 1974.
- [39] S. D. Howison, Complex variable methods in Hele-Shaw moving boundary problems, *Eur. J. Appl. Math*, **3**, 209 (1992).
- [40] L. R. Ford, *Automorphic functions* (McGraw-Hill, New York, 1929); 2nd ed., AMS Chelsea Publ., New York, 1951.
- [41] The expression for $c_l(t)$ is not given here, as it is irrelevant for the velocity field.
- [42] We do not present the expression for Δ , as it is irrelevant for the purposes of this article.
- [43] When an interface approaches a point β_k , it gets ‘pinned’ at this point and expands laterally, leaving behind a narrow channel of viscous fluid resembling a *fjord*.
- [44] M. Mineev-Weinstein and S. P. Dawson, Class of nonsingular exact solutions for Laplacian pattern formation, *Phys. Rev. E* **50**, R24 (1994).
- [45] M. Mineev-Weinstein and S. P. Dawson, Long-time behavior of the N-finger solution of the Laplacian growth equation, *Physica D* **73**, 373 (1994).
- [46] M. D. Kruskal and H. Segur, ARAP Tech. Memo (unpublished), 1985.
- [47] M. D. Kruskal and H. Segur, Asymptotics beyond all orders in a model of crystal growth, *Stud. Appl. Math*, **85**, 129 (1991).
- [48] S. Tanveer, The effect of surface tension on the shape of a Hele-Shaw cell bubble, *Phys. Fluids* **29**, 3537 (1986).
- [49] S. Tanveer, New solution for steady bubbles in a Hel-Shaw cell, *Phys. Fluids* **30**, 651 (1987).
- [50] E. Pauné, F. X. Magdaleno, and J. Casademunt, Dynamical systems approach to Saffman-Taylor fingering: Dynamical solvability scenario, *Phys. Rev. E* **65** 056213 (2002).
- [51] J. Casademunt, Viscous fingering as a paradigm of interfacial pattern formation: Recent results and new challenges, *Chaos* **14**, 809 (2004).
- [52] S. J. Chapman and J. R. King, The selection of Saffman-Taylor fingers by kinetic undercooling, *J. Eng. Math.*, **46**, 1 (2003).
- [53] M. Dallaston and S. McCue, Numerical solution to the Saffman-Taylor finger problem with kinetic undercooling regularisation, *ANZIAM J*, **52**, C124 (2011).
- [54] A. P. Aldushin and B. J. Matkowsky, Selection in the Saffman-Taylor finger problem and the Taylor-Saffman bubble problem without surface tension, *Appl. Math. Lett.* **11**, 57 (1998).

- [55] M. J. Feigenbaum, Pattern selection: determined by symmetry and modifiable by distant effects. *J. Stat. Phys.* **112**, 219 (2003).
- [56] D. Crowdy and S. Tanveer, The effect of finiteness in the Saffman-Taylor viscous fingering problem, *J. Stat. Phys.* **114**, 1501 (2004).